Energy Reports 4 (2018) 274–287

Contents lists available at ScienceDirect

Energy Reports

journal homepage: www.elsevier.com/locate/egyr

Research paper

# Modeling, simulation and performance analysis of solar PV array configurations (Series, Series–Parallel and Honey-Comb) to extract maximum power under Partial Shading Conditions

Suneel Raju Pendem, Suresh Mikkili *

*Department of Electrical and Electronics Engineering, National Institute of Technology Goa, India*

## HIGHLIGHTS

- Series (S), Series-Parallel (S–P) and Honey-Comb (H-C) PV array configurations are modelled.
- Various shading conditions are considered to compare the performance of PV array configurations.
- As the number of PV modules shaded per string and the number of strings shaded in a PV array increases, the maximum power generation capability decreases.
- The maximum power generated and mismatching power loss is calculated under all shading conditions for each PV array configuration.
- Honey-Comb (H-C) PV array configuration is the most appropriate PV configuration for the generation of maximum power compared to Series (S) and Series-Parallel (S–P) PV array configurations.

## ARTICLE INFO

*Article history:*
Received 12 September 2017
Received in revised form 14 February 2018
Accepted 22 March 2018
Available online 9 April 2018

*Keywords:*
Maximum Power Point (MPP)
Series (S), Series–Parallel (S–P), Honey-Comb (H-C) PV array configurations
Partial Shading Conditions (PSCs)
Mismatching power loss and Fill Factor (FF)

## ABSTRACT

The main design objective of the solar photovoltaic (PV) systems is to extract the maximum power from the PV systems for a long time. The amount of power extracted from the PV array can be affected by temperature, solar irradiation, dust accumulation, wind speed, PV array configuration and shading pattern. Often, the PV arrays are completely or partially shadowed and has been recognized as a major challenging concern which can reduce the output power of PV arrays due to mismatching power loss between the PV modules and also represents multiple Maximum Power Points (MPPs) in the electrical characteristics (I–V and P–V characteristics). The key objectives of this paper are to model, simulate and study the effects of PSCs on the electrical characteristics of Series (S), Series–Parallel (S–P) and Honey-Comb (H-C) PV array configurations under various shading patterns such as, short and narrow, short and wide, long and narrow, long and wide, and diagonal shading patterns by using a MATLAB/Simulink simulation model. The performance analysis of the PV array configurations is carried out by considering the maximum power generated ($P_{MP}$), open-circuit voltage ($V_{OC}$), voltage at maximum power point ($V_{MPP}$), short-circuit current ($I_{SC}$), current at maximum power point ($I_{MPP}$), mismatching power loss ($\Delta P_L$) and fill factor (FF). The simulation and performance analysis of PV array configurations is performed with 25 PV modules of KYOCERA-KC200GT modules.



## 1. Introduction

The ever-growing demand for a low-cost energy and an increasing concern about environmental issues has motivated an enormous attention in the utilization of freely and abundantly available renewable energy sources such as solar, wind tidal energy etc. Among these renewable energy sources, solar Photovoltaic (PV) systems has attracted more attention due to the decrease in the price of PV modules, intentional government subsidies and innovative business models in the residential, commercial and utility power systems (Essakiappan et al., 2011). The solar energy can be easily converted into electrical energy using PV cells/modules/arrays. The performance and efficiency of PV systems depend on many factors; such as solar irradiation, temperature, aging effect, potential induced degradation effects etc. In general, the variations in solar irradiation and temperature will be

* Corresponding author.
*E-mail addresses:* psuneelraju.eee@gmail.com (S.R. Pendem), mikkili.suresh@nitgoa.ac.in (S. Mikkili).

https://doi.org/10.1016/j.egyr.2018.03.003

**Nomenclature**

**Abbreviations**

| | |
|---|---|
| PV system | Photovoltaic system |
| PSCs | Partial Shading Conditions |
| MPP | Maximum Power Point |
| MPPT | Maximum Power Point Tracking |
| S | Series |
| S–P | Series–Parallel |
| H-C | Honey-Comb |
| FF | Fill Factor |

**Symbols**

| | |
|---|---|
| $P_{MP}$ | Power generated at maximum power point [W] |
| $P_{PV}$ | Power generated in a PV array [W] |
| $I_{MP}$ | Current at maximum power point [A] |
| $I_{PH}$ | Photocurrent generated due to solar irradiation [A] |
| $I_{PV}$ | PV array terminal current [A] |
| $I_D$ | Shockley diode current [A] |
| $I_o$ | Terminal current of the PV module [A] |
| $I_r$ | Diode reverse saturation current [A] |
| $I_{SH}$ | Current flowing through the shunt resistance [A] |
| $I_j$ | Current flowing through a PV module [A] |
| $V_{MP}$ | Voltage at maximum power point [V] |
| $V_{PV}$ | PV array terminal Voltage [V] |
| $V_T$ | Thermal voltage of the PV module [V] |
| $V_o$ | Terminal Voltage of the PV module [V] |
| $V_D$ | Voltage across the diode [V] |
| $V_j$ | Voltage across a PV module [V] |
| $G$ | Solar irradiance [W/m$^2$] |
| $T$ | Module operating temperature [K] |
| $R_S$ | Series resistance of the PV module [Ω] |
| $R_{SH}$ | Shunt resistance of the PV module [Ω] |
| $N_S$ | Number of modules connected in series |
| $N_P$ | Number of modules connected in parallel |
| $n_s$ | Number of cells in series in a PV module |
| $J$ | Total number of modules in a PV array |
| $K$ | Boltzmann's constant $= 1.380 \times 10^{-23}$ J/K |
| $m$ | Number of rows in a PV array |
| $n$ | Number of columns (strings) in a PV array |
| $q$ | Charge of the electron $= 1.602 \times 10^{-19}$ C |
| $a$ | Diode emission coefficient or ideality factor |

considered as the most affecting factors of PV generation systems. The temperature has an enormous effect on aging of PV modules. If the PV modules are subjected to higher temperatures, it can lead to module delamination, creation of bubbles, corrosion etc. (Manganiello et al., 2015). Under uniform irradiation condition (i.e., all the cells in a module or array receives the same irradiation), PV systems represents a unique Maximum Power Point (MPP) in the non-linear $I$–$V$ and $P$–$V$ characteristics. This MPP can be tracked by employing conventional Maximum Power Point Tracking (MPPT) techniques (Eltawil et al., 2013; Verma et al., 2014).

Under the Partial Shading Conditions (PSCs), commonly referred to as mismatching conditions, certain cells or modules in a PV array are shaded by passing clouds, trees, poles, buildings, bird droppings and some other objects (Murtaza et al., 2014). Therefore, under PSCs PV modules represent multiple maximum power points (MPPs) in the non-linear $I$–$V$ and $P$–$V$ characteristics. The presence of multiple MPPs in the $I$–$V$ and $P$–$V$ characteristics can mislead conventional MPPT techniques, and to track the global MPP, soft computing based MPPT techniques are efficient (Ahmed et al., 2015; Murtaza et al., 2014). Due to PSCs, PV systems are prone to mismatching power losses, and hence the maximum power generation capability and efficiency of PV systems decreases. In addition due to PSCs, the mismatching power losses in a PV system are also due to dust and soiling, defects of bypass diodes, different positioning of the PV modules in the same string with respect to solar irradiation, differences between the PV cells physical parameters, manufacturing tolerances etc. (Manganiello et al., 2015). These mismatching power losses in a PV system can be reduced by employing various approaches; these are PV array configurations, PV system architectures, MPPT techniques, and converter circuit topologies.

PV array configuration is one of the finest keys that can considerably decreases the mismatching and power losses under PSCs. It is based on the various electrical interconnection techniques between the PV modules (Belhachat and Larbes, 2015). The PV system architecture describes the various approaches of integrating power electronic converters to PV systems, i.e., central inverter configuration, cascaded DC–DC converters with central inverter configuration and micro-inverter configuration etc. (Bhatnagar and Nema, 2013). The MPPT techniques (i.e., centralized MPPT, distributed MPPT, reconfiguration MPPT, module-level MPPT techniques and etc.) are implemented to extract the maximum possible power from the PV systems under uniform and PSCs. The module-level MPPT is the advanced technique of power electronic converters (Chao et al., 2015; Quesada et al., 2009; Rani et al., 2013). The different types of converter circuit topologies to PV systems for grid integration are reported in Dhople et al. (2010), Koutroulis et al. (2012) and Roman et al. (2006).

During Partial Shading Conditions (PSCs), PV systems represent multiple MPPs in output characteristics which are explained in Section - 4 validated with the simulation results. Due to PSCs, PV systems produce mismatching power losses, and hence the maximum power generation capability and efficiency of PV system decreases. The PV array topology is one of the finest keys that can considerably decreases the mismatching power losses under PSCs. Some researchers have attempted the following approaches to mitigate the mismatching power losses in PV systems.

### 1.1. Comparison of various PV array topologies

- Patel and Agarwal (2008) detailed a brief comparison of large connected S and S–P PV array topologies under PSCs. The modeling and analysis of S and S–P PV array topologies is based on MATLAB/Simulink software. The results prove that the magnitude of global peak power is dependent on the PV array topology and the shading pattern.
- Belhachat and Larbes (2015) detailed a brief comparison of various PV array topologies under row and column shading patterns. The results prove that the performance of T–C–T PV array topology is better under row and column shading patterns.
- Wang and Hsu (2011) studied and compared the performance of five different topologies of PV cells (S, S–P, T–C–T, B–L and H-C) under PSCs. The analysis of PV array topologies is followed by solving the simultaneous nonlinear equations using the Newton–Raphson algorithm.
- Ramaprabha and Mathur (2012) reviewed and developed a generalized MATLAB M-code to compare and investigate the effects of PSCs on various PV array topologies.

### 1.2. Advanced proposed PV array topologies

- Bhatnagar and Nema (2013) reviewed various Maximum Power Point Tracking (MPPT) algorithms that are implemented in the power conversion devices to extract the maximum power from the array by forcing input impedance of the power conversion devices to match the MPP of the PV array.
- Chao et al. (2015) proposed an adaptive reconfiguration technique to PV modules in an array under PSCs and malfunctioning conditions. In this technique, the PV modules in the array are divided into fixed end and adaptive bank. When the PV modules in the fixed end are shaded or malfunctioned, these modules are connected to those modules in the adaptive bank. To implement this technique a large number of switches and sensors are required.
- Quesada et al. (2009) proposed a dynamic reconfiguration strategy that can be implemented to Building Integrated Photovoltaic Systems and to large PV systems affected by passing clouds. To implement this technique high cost and greater complexity are involved.
- Rani et al. (2013) proposed a new a technique to extract the maximum power under PSCs. In this technique the physical location of the PV modules in the array is connected by employing T–C–T PV array configuration, but all the PV modules are arranged based on Su Do Ku puzzle pattern. The drawback of this technique is ineffectual distribution of shade and significant rise in wiring requirements.

### 1.3. Power electronics based techniques to extract maximum power

- Roman et al. (2006) proposed Micro-inverter MPPT architecture to extract maximum power than string-level or array level inverter. In this architecture each PV module has its own inverter along with a MPPT and all the micro-inverter outputs are connected to the common AC bus. The disadvantage of this technique is the cost of micro-inverter is higher.
- Dhople et al. (2010) proposed a multiple-input boost converter topology to implement MPPT for series strings of solar cells connected across bypass diodes in a PV module. The proposed topology can be adopted in distributed MPPT system architectures that utilize micro-inverters.
- Koutroulis et al. (2012) proposed a new MPPT technique for tracking the GMPP of PV arrays operating under PSCs using D-flip/flop and analog/digital converter approach.

So, compared with the previous research works to select the best PV array configuration, the key objective of this research article is to model, simulate and to the analyze the performance of Series (S), Series–Parallel (S–P) and Honey-Comb (H-C) PV array configurations under different PSCs by simulating 5 × 5 PV array in MATLAB/SIMULINK without considering any physical relocation of PV modules. The performance analysis of PV array configurations is carried out under different PSCs such as, short and narrow shading, short and wide shading, long and narrow shading, long and wide shading, and diagonal shading. The performance analysis of these configurations are referred with respect to the maximum generated values of powers, voltages, currents, mismatching losses and fill factor (FF). This will provide one of the key solutions to select the best PV array configuration under PSCs.

This research article is organized as follows: Section 2 describes the modeling of PV array in MATLAB/SIMULINK; different types of shading conditions and its solar irradiance levels are described inSection 3; modeling and simulation of PV array configurations are provided in Section 4; the analysis and performance evaluation of PV array configurations are described in Section 5; conclusion is given in Section 6.

## 2. Mathematical modeling of PV module in MATLAB/Simulink

The PV cell is the main component of PV system which converts solar PV energy into electrical energy. Generally, the Silicon PV cell has an open-circuit voltage of 0.7 V and maximum power generation capability of 1 to 5 W. PV cells are made of several types of semiconductor materials using various manufacturing processes. At present, the mono-crystalline and poly-crystalline silicon cells are mostly used for manufacturing the PV modules. The series connection of PV cells forms a PV module. The specifications of any PV module are considered as maximum power ($P_{MP}$ (W)), open-circuit voltage ($V_{oc}$ (V)), short-circuit current ($I_{SC}$ (A)), voltage at MPP ($V_{MP}$ (V)), current at MPP ($I_{MP}$ (A)), series resistance ($R_S$ (Ω)), shunt resistance ($R_{SH}$ (Ω)), number of series cells per module ($N_S$), temperature coefficient of open-circuit voltage ($K_V$ (V/Kelvin)) and temperature coefficient of short-circuit current ($K_I$ (A/Kelvin)). The practical equivalent circuit of PV module in MATLAB/Simulink model is shown in Fig. 1(a) (Villalva et al., 2009). The amount of power generated from the PV cell or module mainly depends on the solar irradiation ($G$ (W/m$^2$) and temperature ($T$ (Kelvin)). Fig. 1(b) shows the MATLAB/Simulink subsystem model of PV module simulated at Standard Test Condition (STC) of 1000 W/m$^2$ and 25°C. The simulated output power, voltage, current, and $I$–$V$ and $P$–$V$ characteristics of PV module can be obtained with $N_S$ cells connected in series is represented in Fig. 1(c).

■ The basic mathematical equation describing the $I$–$V$ characteristics of practical PV module is given by Eq. (1).

$$I_o = I_{PH} - I_r\left[\exp\left(\frac{V_o + R_S I_o}{V_T a}\right) - 1\right] - \frac{V_o + R_S I_o}{R_{SH}}$$
$$= I_{PH} - I_r\left[\exp\left(\frac{q(V_o + R_S I_o)}{n_s K T a}\right) - 1\right] - \frac{V_o + R_S I_o}{R_{SH}} \quad (1)$$

where $I_{PH}, I_r$ *and* $I_o$ are the photo generated current due to incident solar irradiation [A], diode reverse leakage current [A] and terminal current of the PV module [A]; $V_o$ *and* $V_T = (n_s \times K \times T)/q$ are the terminal voltage and thermal voltage of the PV module [V]; $K$ is Boltzmann's constant ($1.380 \times 10^{-23}$ J/K); $T$ is the module operating temperature (Kelvin); $q$ is charge of the electron ($1.602 \times 10^{-19}$ C); $R_S$ *and* $R_{SH}$ are the series and shunt resistances of the PV module; and $a$ is the diode emission coefficient. The ideal value of diode emission coefficient is 1. The different techniques of estimating the exact the value of '$a$' are presented in Pongratananukul et al. (2004).

■ The photo generated current of the PV module $I_{PH}$ is linearly depends on the incident solar irradiation and is also influenced by the temperature according to the Eq. (2).

$$I_{PH} = \frac{G}{G_{STC}}\left(I_{PH,STC} + K_I \Delta_T\right) \quad (2)$$

where $G_{STC}$ (W/m$^2$) is the irradiation at STC; $G$ is the irradiation on the surface of PV module; $I_{PH,STC}$ (A) is the photo generated current at STC; $K_I$ is the temperature coefficient of the short-circuit current (A/Kelvin) and $\Delta_T = T - T_{STC}$ ($T$ and $T_{STC}$ are the actual and STC temperatures (Kelvin)).

■ The diode reverse leakage current $I_r$ is strongly depends on the temperature and is given in Eq. (3).

$$I_r = \frac{I_{SC,STC} + K_I \Delta_T}{\exp\left(\left(V_{OC,STC} + K_V \Delta_T\right)/aV_T\right) - 1} \quad (3)$$

where $I_{SC,STC}$ (A) and $V_{OC,STC}$ (V) is the short-circuit current and open-circuit voltage at STC; $K_V$ is the temperature coefficient of open-circuit voltage (V/Kelvin).

From Eq. (1), to describe the relationship between the PV module terminal current and voltage of PV module, the values of the parameters $R_S$ and $R_{SH}$ has to be estimate. In the literature Dhople et al. (2010) proposed iterative solutions method and Villalva et

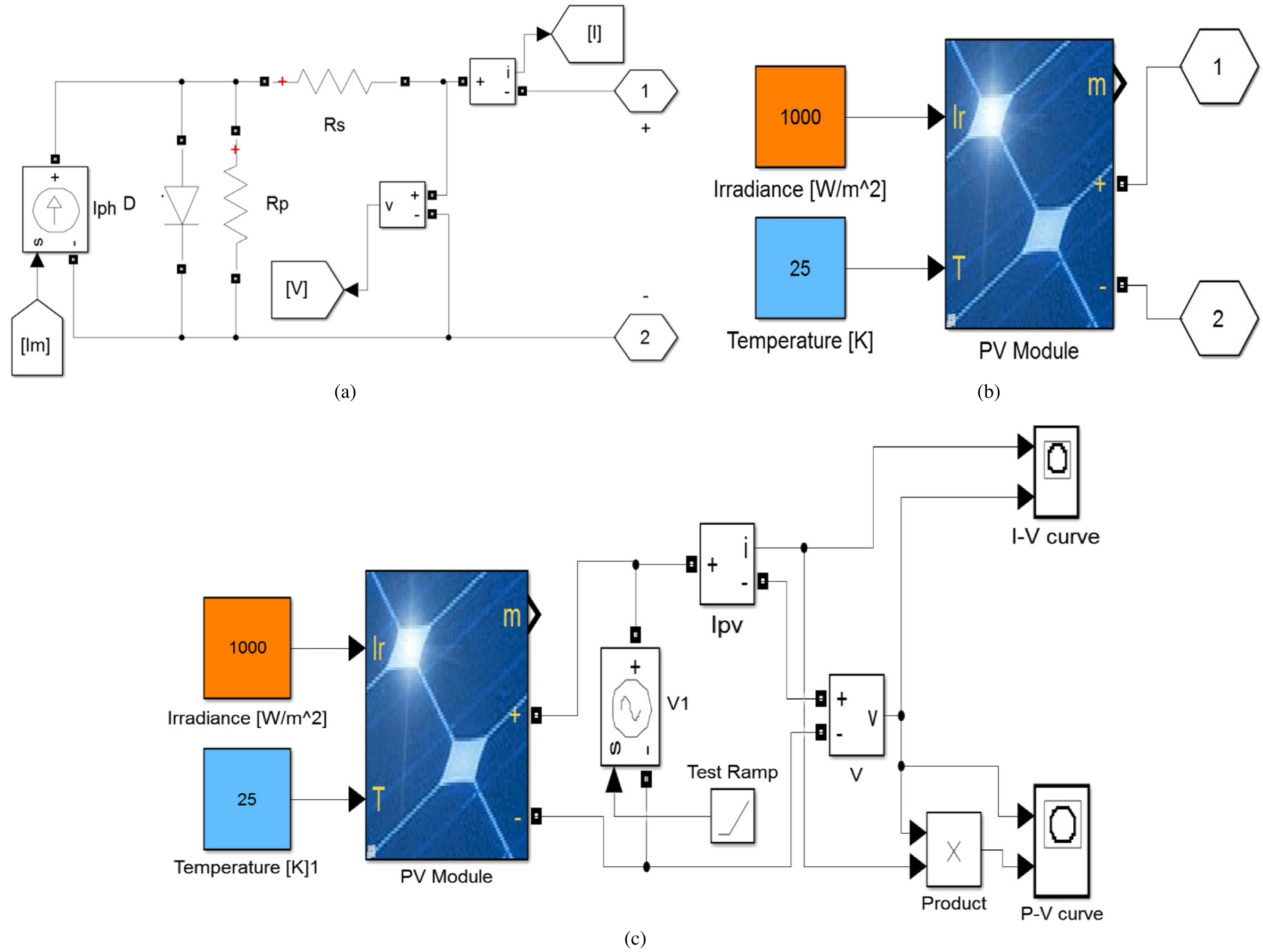


**Fig. 1.** PV module modeling in MATLAB/Simulink. (a) Equivalent circuit of PV Module, (b) Subsystem model of PV module and (c) PV module simulation for output power, voltage, current and $I$–$V$ and $P$–$V$ characteristics.

al. (2009) proposed maximum power matching method which is used in this paper to estimate the values of $R_S$ and $R_{SH}$. In both the methods, the following three operating conditions of the PV module are considered:

**(a) Open-circuit condition:** In this condition the output terminals of the PV module are open-circuited; hence the voltage across the PV module '$V_0$' is equal to the open-circuit voltage $V_{OC}$ ($V_0 = V_{OC}$) and the terminal current of the PV module $I_0 = 0$ which is given in Eq. (4).

$$0 = I_{PH} - I_r\left[\exp\left(\frac{V_{OC}}{V_T a}\right) - 1\right] - \frac{V_{OC}}{R_{SH}}. \tag{4}$$

**(b) Short-circuit condition:** In this condition the output terminals of the PV module are short-circuited; hence the voltage across the PV module '$V_0$' is equal to zero ($V_0 = 0$) and the terminal current of the PV module is equal to $I_{SC}$ ($I_0 = I_{SC}$) which is given in Eq. (5).

$$I_{SC} = I_{PV} - I_r\left[\exp\left(\frac{I_{SC}R_S}{V_T a}\right) - 1\right] - \frac{I_{SC}R_S}{R_{SH}}. \tag{5}$$

**(c) Maximum power point condition:** In this operating condition, the current flowing through the output terminals of the PV module is equal to $I_o = I_{MP}$ and the voltage across the PV module is equal to $V_0 = V_{MP}$. In addition, the variation of power with respect to variation in voltage at MPP is equal to zero, i.e. $\frac{dP_{MP}}{dV_{MP}} = 0$ which is given in Eq. (6).

$$I_{MP} = I_{PV} - I_r\left[\exp\left(\frac{V_{MP} + I_{MP}R_S}{V_T a}\right) - 1\right] - \frac{V_{MP} + I_{MP}R_S}{R_{SH}}. \tag{6}$$

According to the maximum power matching, the maximum power ($P_{max,c}$) calculated by the $I$–$V$ model of (1) is matched to the maximum experimental power ($P_{max,e}$) from the data sheet at MPP and solving for $R_S$ gives Eq. (7).

$$\begin{aligned} P_{max,c} &= V_{MP}\left\{I_{PV} - I_r\left[\exp\left(\frac{V_{MP} + I_{MP}R_S}{V_T a}\right) - 1\right] - \frac{V_{MP} + I_{MP}R_S}{R_{SH}}\right\} \\ &= P\ \max,e \end{aligned} \tag{7}$$

$$R_{SH} = \frac{V_{MP} + I_{MP}R_S}{\left\{V_{MP}I_{PV} + V_{MP}I_o - V_{MP}I_o \exp\left[\frac{q(V_{MP}+I_{MP}R_S)}{N_s KTa}\right] - P_{max,e}\right\}} \tag{8}$$

From Eq. (8), it is clear that for any value of $R_S$ there will be a value of $R_{SH}$. To find the value of $R_S$ (and hence, $R_{SH}$), the MPP of mathematical $I$–$V$ curve coincides to the experimental MPP. This requires several iterative solutions until $P_{max,c} = P_{max,e}$.

■ The $I$–$V$ and $P$–$V$ characteristics of PV module operating at constant temperature of 25 °C and various irradiance levels are given in Fig. 2(a) and (b).

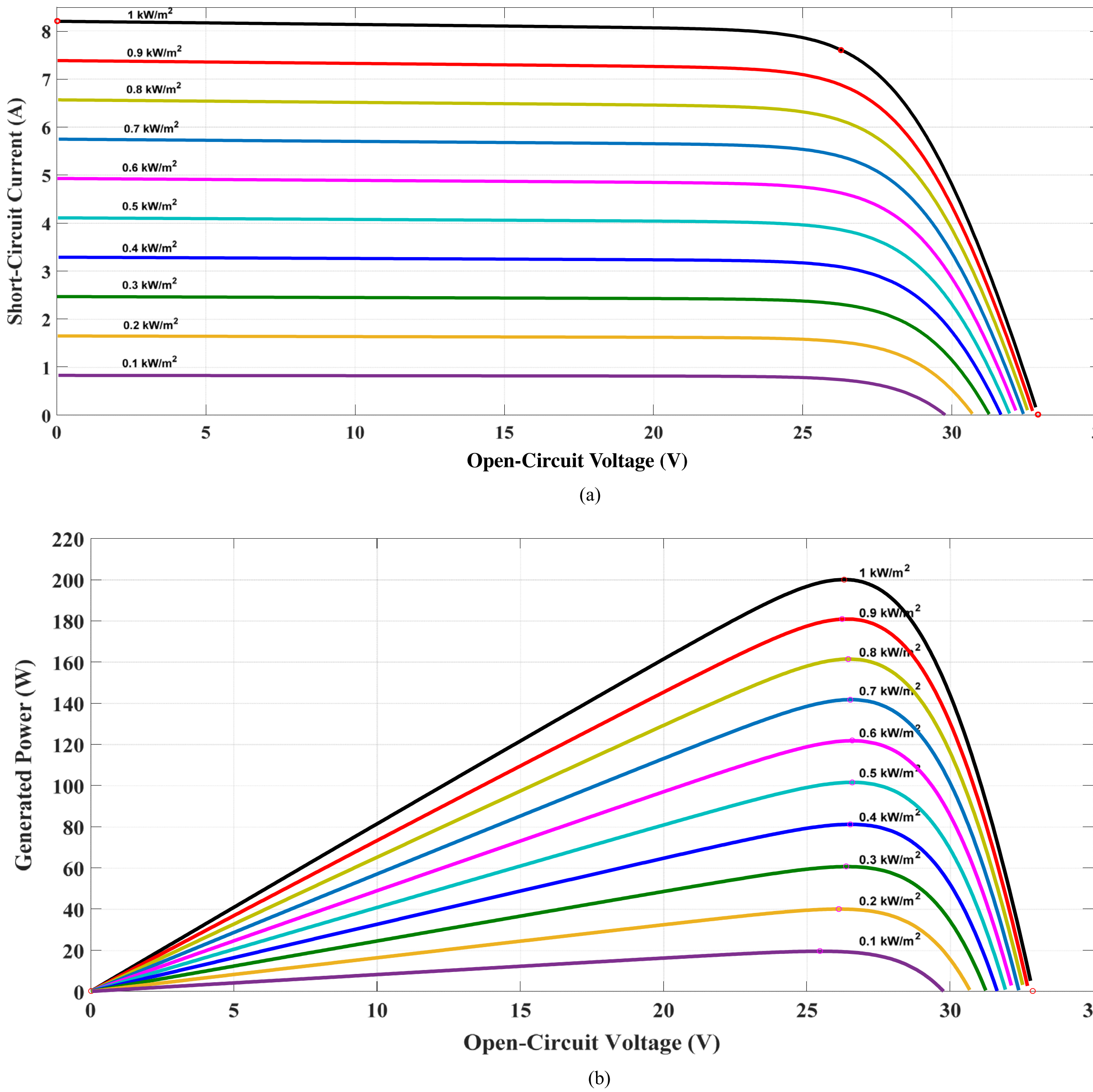


**Fig. 2.** Output characteristics of PV module under various irradiation levels (a) $I$–$V$ characteristics and (b) $P$–$V$ characteristics.

## 3. Description of partial shading conditions on PV array configurations

In this section, different types of shading conditions on S, S–P and H-C configurations are presented and are subjected constant irradiation levels on each PV module. In a PV array, based on the number of shaded modules per string (column) and number of shaded strings, shading conditions are classified into four types as; short and narrow; short and wide; long and narrow; and long and wide shading conditions. Another shading condition, i.e. diagonal shading in which the solar irradiance levels are varying in diagonal pattern is also considered. For each shading condition the simulated output characteristics of PV array configurations are explained in section.4. The description of each shading condition and solar irradiance levels on 5 × 5 PV array configurations is given as follows.

### 3.1. Short and narrow shading condition

In short and narrow shading condition, only two strings are shaded out of five strings (narrow compared to width of the PV array) and the number of modules shaded per string is three (short compared to length of the string), hence this shading condition is referred to as short and narrow shading condition. To evaluate the performance of the PV configurations under PSCs, solar irradiance levels are categorized into four different groups. The varying solar irradiance level under short and narrow shading is represented in Table 1.

- Group 1: Modules — 2, solar irradiance — 300 W/m$^2$
- Group 2: Modules — 2, solar irradiance — 500 W/m$^2$
- Group 3: Modules — 2, solar irradiance — 700 W/m$^2$
- Group 4: Modules — 19, solar irradiance — 1000 W/m$^2$.

### 3.2. Short and Wide shading condition

When four strings are shaded out of five strings (wide compared to width of the PV array) and the number of modules shaded per string is three, this condition is referred to as short and wide shading condition. Here also, the solar irradiance levels are categorized into four different groups. The varying solar irradiance level under short and wide shading is represented in Table 2.

**Table 1**
Short and narrow shading condition.

| | $S_1$ | $S_2$ | $S_3$ | $S_4$ | $S_5$ |
|---|---|---|---|---|---|
| $R_1$ | 300 | 300 | 1000 | 1000 | 1000 |
| $R_2$ | 500 | 500 | 1000 | 1000 | 1000 |
| $R_3$ | 700 | 700 | 1000 | 1000 | 1000 |
| $R_4$ | 1000 | 1000 | 1000 | 1000 | 1000 |
| $R_5$ | 1000 | 1000 | 1000 | 1000 | 1000 |

**Table 2**
Short and wide shading condition.

| | $S_1$ | $S_2$ | $S_3$ | $S_4$ | $S_5$ |
|---|---|---|---|---|---|
| $R_1$ | 300 | 300 | 500 | 500 | 1000 |
| $R_2$ | 300 | 300 | 500 | 500 | 1000 |
| $R_3$ | 700 | 700 | 700 | 700 | 1000 |
| $R_4$ | 1000 | 1000 | 1000 | 1000 | 1000 |
| $R_5$ | 1000 | 1000 | 1000 | 1000 | 1000 |

**Table 3**
Long and narrow shading condition.

| | $S_1$ | $S_2$ | $S_3$ | $S_4$ | $S_5$ |
|---|---|---|---|---|---|
| $R_1$ | 300 | 300 | 1000 | 1000 | 1000 |
| $R_2$ | 300 | 500 | 1000 | 1000 | 1000 |
| $R_3$ | 500 | 500 | 1000 | 1000 | 1000 |
| $R_4$ | 700 | 700 | 1000 | 1000 | 1000 |
| $R_5$ | 700 | 700 | 1000 | 1000 | 1000 |

**Table 4**
Long and wide shading condition.

| | $S_1$ | $S_2$ | $S_3$ | $S_4$ | $S_5$ |
|---|---|---|---|---|---|
| $R_1$ | 300 | 300 | 500 | 500 | 1000 |
| $R_2$ | 300 | 300 | 500 | 500 | 1000 |
| $R_3$ | 300 | 300 | 500 | 500 | 1000 |
| $R_4$ | 700 | 700 | 900 | 900 | 1000 |
| $R_5$ | 700 | 700 | 900 | 900 | 1000 |

- Group 1: Modules – 4, solar irradiance – 300 W/m$^2$
- Group 2: Modules – 4, solar irradiance – 500 W/m$^2$
- Group 3: Modules – 4, solar irradiance – 700 W/m$^2$
- Group 4: Modules – 13, solar irradiance – 1000 W/m$^2$.

### 3.3. Long and narrow shading condition

Two strings are shaded out of 5 strings and all the modules per string are shaded (long compared to length of the string), so this shading condition is referred as long and narrow shading condition. The solar irradiance levels in a PV are categorized into four different groups. The varying solar irradiance levels under long and narrow shading are represented in Table 3.

- Group 1: Modules – 3, solar irradiance – 300 W/m$^2$
- Group 2: Modules – 3, solar irradiance – 500 W/m$^2$
- Group 3: Modules – 4, solar irradiance – 700 W/m$^2$
- Group 4: Modules – 15, solar irradiance – 1000 W/m$^2$.

### 3.4. Long and wide shading condition

The four strings of the PV array are shaded out of five strings and all the modules in string are shaded, and referred to as long and narrow shading condition. In this shading condition, the solar irradiance levels are categorized into five groups. The varying solar irradiance levels under long and wide shading are represented in Table 4.

**Table 5**
Diagonal shading condition.

| | $S_1$ | $S_2$ | $S_3$ | $S_4$ | $S_5$ |
|---|---|---|---|---|---|
| $R_1$ | 300 | 1000 | 1000 | 1000 | 1000 |
| $R_2$ | 1000 | 400 | 1000 | 1000 | 1000 |
| $R_3$ | 1000 | 1000 | 500 | 1000 | 1000 |
| $R_4$ | 1000 | 1000 | 1000 | 700 | 1000 |
| $R_5$ | 1000 | 1000 | 1000 | 1000 | 900 |

- Group 1: Modules – 6, solar irradiance – 300 W/m$^2$
- Group 2: Modules – 6, solar irradiance – 500 W/m$^2$
- Group 3: Modules – 4, solar irradiance – 700 W/m$^2$
- Group 4: Modules – 4, solar irradiance – 900 W/m$^2$.
- Group 5: Modules – 5, solar irradiance – 1000 W/m$^2$.

### 3.5. Diagonal shading condition

The five diagonally placed PV modules in a PV array are subjected to different solar irradiance levels. The solar irradiance levels on diagonally placed PV modules are considered as 300 W/m$^2$, 400 W/m$^2$, 500 W/m$^2$, 700 W/m$^2$ and 900 W/m$^2$ respectively and are represented in Table 5.

## 4. Modeling and simulation of PV array configurations under PSCs

This section describes the modeling and simulation of following three 5 × 5 PV array configurations under short and narrow, short and wide, long and narrow, long and wide, and diagonal shading conditions.

- Series (S) PV array
- Series–Parallel (S–P) PV array and
- Honey-Comb (H-C) PV array.

For the simulation of above 5 × 5 PV array topologies 25 PV modules are used. Each PV module and string is protected by anti-parallel bypass diode and series connected blocking diodes. These PV modules operate at constant temperature of 25 °C and various irradiation levels as described in Section 3. The specifications of Kyocera-KC200GT PV module are given in Appendix.

### 4.1. Series PV array configuration (S)

The MATLAB/Simulink model of 5 × 5 series PV array configuration is shown in Fig. 3a. In this configuration all the PV modules are connected in series connection. In series connection, the PV array current is same as module current or cell current and the array voltage is equivalent to sum of the voltages of the individual PV modules. Under PSCs, the series PV array current is limited by the lowest irradiance level and non-linear output characteristics of PV cells or modules are prone to mismatching power losses. Therefore, shaded modules operate in reverse bias condition to generate the short circuit current equal to unshaded PV modules. Since, the shaded modules operates in reverse bias condition, instead of delivering power they will dissipates the power in the form of heat and causes hot spots which damages the PV modules.

In order for the safe operation of PV modules from hot spot effects, to each PV module bypass diodes are connected in anti-parallel (Mäki et al., 2012; Pongratananukul et al., 2004). Under

PSCs; PV modules receive distinct irradiance and forward bias the bypass diodes. These diodes share portion of the short circuit current of the shaded modules and represents multiple I–V and P–V characteristics in a single *I–V* and *P–V* characteristics. The simulated *I–V* and *P–V* characteristics of series (S) PV array configuration under various shading patterns are shown in Figs. 3b and 3c.

### 4.2. Series–parallel PV array configuration (S–P)

In Series–Parallel (S–P) PV array configuration — the PV modules are first connected in series to form strings to generate a desired output voltage and then these strings are connected in parallel to generate desired output current (Cipriani et al., 2014). This configuration is most commonly employed because it is easy to construct, economical and there are no redundant connections. The MATLAB/Simulink model of 5 × 5 S–P PV array configuration is shown in Fig. 4a. The PV modules in this configuration are divided into five rows and five strings and each string consists of five series connected modules. The PV array current is the sum of the five string currents and the array voltage is equal to the sum of individual PV module voltages in a string. In Fig. 4a, in addition to bypass diodes, blocking diodes are also connected in series to protect each PV string from severe PSCs or short circuit conditions. These diodes blocks backflow of string current into another string due to the potential difference between the strings under PSCs (Balato et al., 2015). In standalone PV systems, blocking diodes are preferred to block reverse flow of currents from the storage battery to PV array under PSCs or at night times. The simulated *I–V* and *P–V* characteristics of S–P PV array configuration under various shading patterns are shown in Figs. 4b and 4c. Due to more number of series connections in strings, the mismatching losses are also more but less than series PV array configuration.

### 4.3. Honey-comb PV array configuration (H-C)

The disadvantages of S and S–P PV array configuration can overcome by employing H-C PV array configuration (Cipriani et al., 2014). The MATLAB/Simulink model of 5 × 5 H-C PV array topology is shown in Fig. 5a. In this configuration, all the PV modules are interconnected similar to the hexagon shape of the honey comb architecture. The H-C PV array configuration is having more number of electrical connections between the PV modules compared to S and S–P PV array configuration and having less number of series connections compare to S and S–P array configurations. Therefore, the mismatching power losses of H-C PV array configurations are less than S and S–P PV array configurations. The output characteristics of H-C array configuration under different PSCs are shown in Figs. 5b and 5c.

Let $I_J$ and $V_J$ is the module current and voltages in a string, $I_S$ and $V_R$ are the currents and voltages in a string, and $I_0$ and $V_0$ are the PV array current and voltages. The current, voltage and power outputs of all the PV array topologies in terms of module and string currents and voltages are expressed in Table 6.

## 5. Performance analysis of PV array configurations under PSCs

This section describes the performance of S, S–P and H-C PV array configurations under uniform and PSCs to select the best PV array configuration that offers highest performance. The performance of PV array configuration is determined with respect to mismatching losses and fill factor (FF) (Pongratananukul et al., 2004). The mismatching power loss, $\Delta P_L(\%)$ of the PV system is given in Eq. (9).

$$power\ loss,\ \Delta P_L(\%) = \frac{P_{MP} - P_{PSC}}{P_{MP}} \times 100 \quad (9)$$

where $P_{MP}$ denotes the maximum power generated under uniform illumination condition and $P_{PSC}$ is the maximum power generated under PSC. The maximum power ($V_{MP} \times I_{MP}$) generated at a particular PSC is related to the power ($V_{OC} \times I_{SC}$) generated at nominal operating condition by fill factor given in Eq. (10). As the FF value is close to unity, the performance of the PV system is higher.

$$Fill\ Factor,\ FF = \frac{V_{MP} \times I_{MP}}{V_{OC} \times I_{SC}}. \quad (10)$$

Before discussing the performance of PV array configurations under PSCs, we first discuss the performance under uniform irradiance condition.

### 5.1. Uniform irradiance condition (1000 W/m$^2$)

Under uniform irradiance condition, all the PV modules in a 5 × 5 PV array configuration are subjected to an irradiation of 1000 W/m$^2$. From the simulated output characteristics of S, S–P and H-C PV array configurations shown in Figs. 3c, 4c and 5c, all the PV array configurations generates the same maximum power and produces a single MPP on output characteristics which is referred to as a global MPP. The S, S–P and H-C PV array configurations voltages and currents at MPP are: 663.18 V, 7.61 A; 132.63 V, 38.09 A; and 132.63 V, 38.09 A respectively. The maximum generated voltages and currents of S, S–P and H-C PV array configurations are shown in Fig. 6a. Under this condition, the S–P and H-C PV array configurations generates the same voltage and current at maximum power of 5000.23 W. The mismatching losses of S, S–P and H-C configurations are zero and the function of bypass diodes is ignored since all these diodes are operates under reverse bias condition only. The maximum power generated and mismatching losses of S, S–P and H-C PV array configurations are shown in Fig. 6b. The fill factor of S, S–P and H-C PV array configuration is 0.75.

### 5.2. Under partial shading conditions

#### 5.2.1. Short and Narrow shading condition

The generated maximum powers, voltages and currents of S, S–P and H-C array configurations under short and narrow shading condition are 4219.3 W, 554.2 V, 7.61 A; 3725.8 W, 117.35 V, 31.74 A; and 3793.5 W, 137.36 V, 27.61 A respectively. Under this shading condition, S-array configuration produces the highest maximum power of 4219.3 W by generating three MPPs on output characteristics as shown in Fig. 3c. The maximum generated voltages and currents of S, S–P and H-C configurations at MPP are shown in Fig. 7a. The mismatching losses produced by S, S–P and H-C array configurations are 16.48%, 26.25% and 24.91% respectively. The maximum power generated and mismatching losses produced by S, S–P and H-C array configurations are shown in Fig. 7b. The fill factors of these configurations are 0.62, 0.55 and 0.56 respectively. From the results, under short and narrow shading condition, it was observed that S- array configuration is the most appropriate configuration for generating the maximum power by reducing mismatching losses.

#### 5.2.2. Short and wide shading condition

The generated maximum powers, voltages and currents of S, S–P and H-C array configurations under short and wide shading condition are 2659.2 W, 475.4 V, 5.59 A; 2740.7 W, 137.25 V, 19.96 A; and 2835.9 W, 138.88 V, 20.19 A respectively. Under this condition, H-C array configuration produces the highest maximum power of 2835.9 W by generating three MPPs on output characteristics as shown in Fig. 5c. The maximum generated voltages and currents of S, S–P and H-C configurations at MPP are shown in Fig. 8a. The mismatching losses produced by S, S–P and H-C array configurations are 47.36%, 45.75% and 43.86% respectively. The maximum

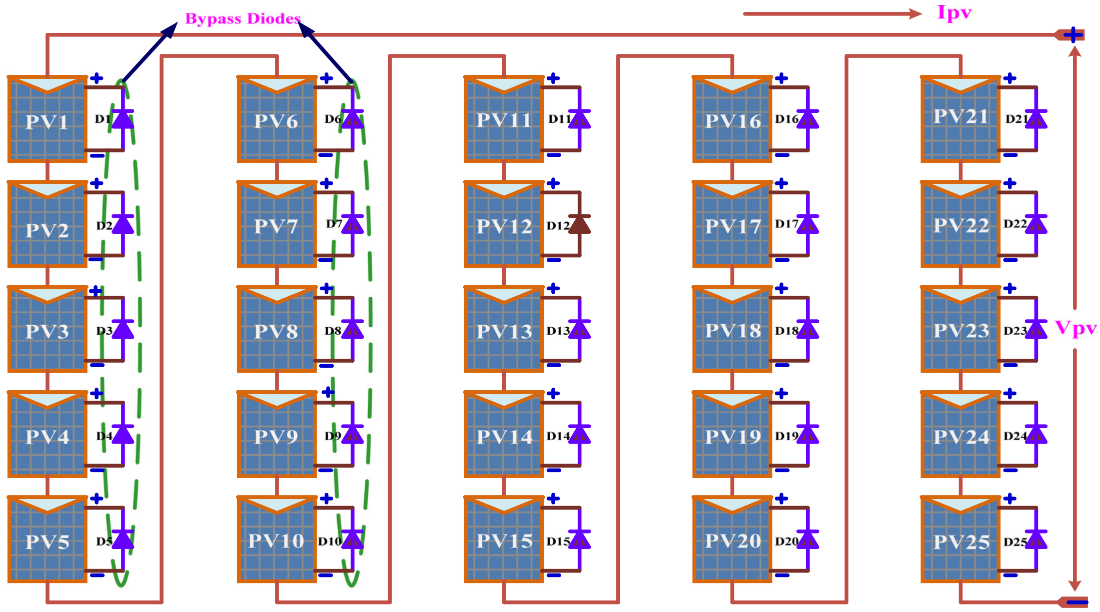


**Fig. 3a.** MATLAB/Simulink model of 5 × 5 series (S) PV array configuration.

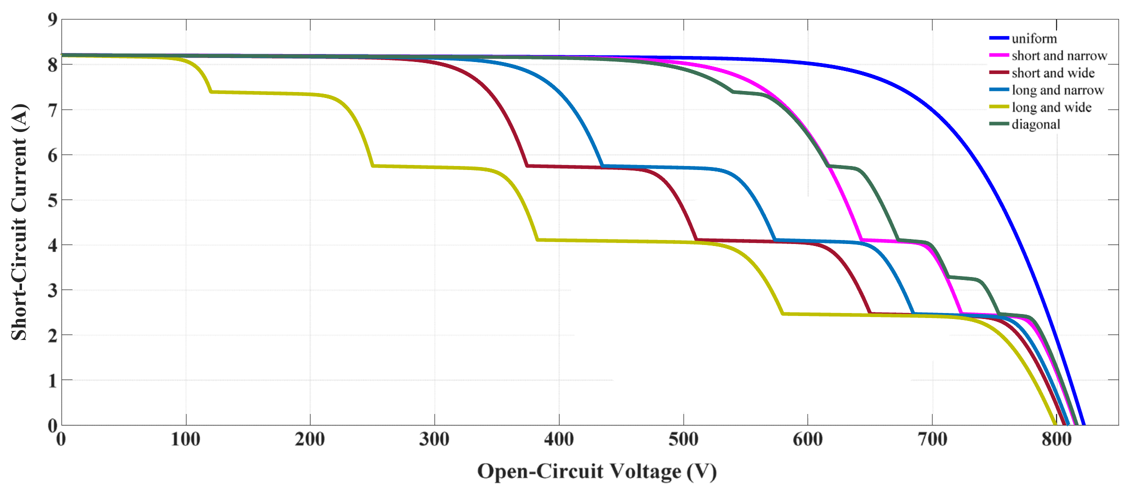


**Fig. 3b.** Simulated *I–V* characteristics of series (S) PV array configuration.

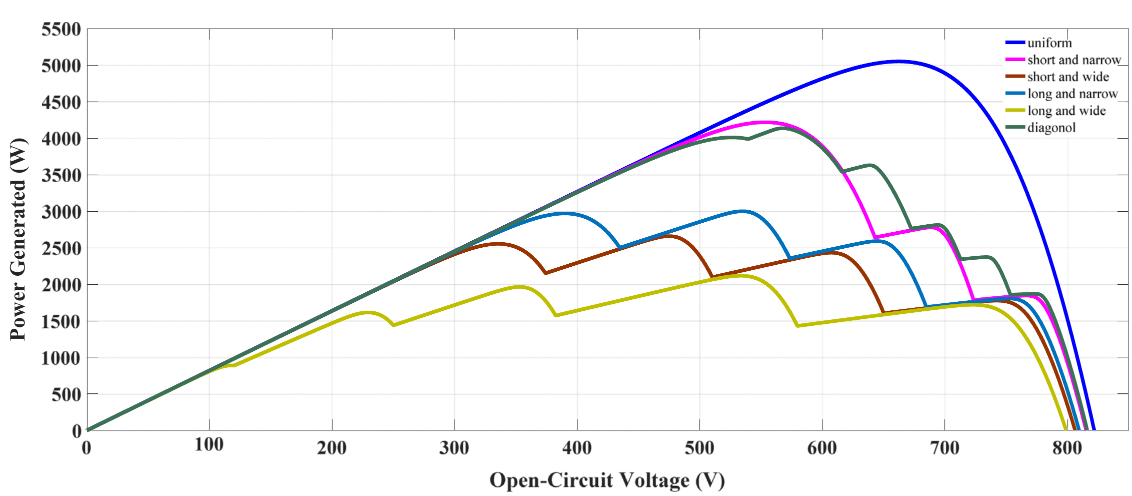


**Fig. 3c.** Simulated *P–V* characteristics of series (S) PV array configuration.

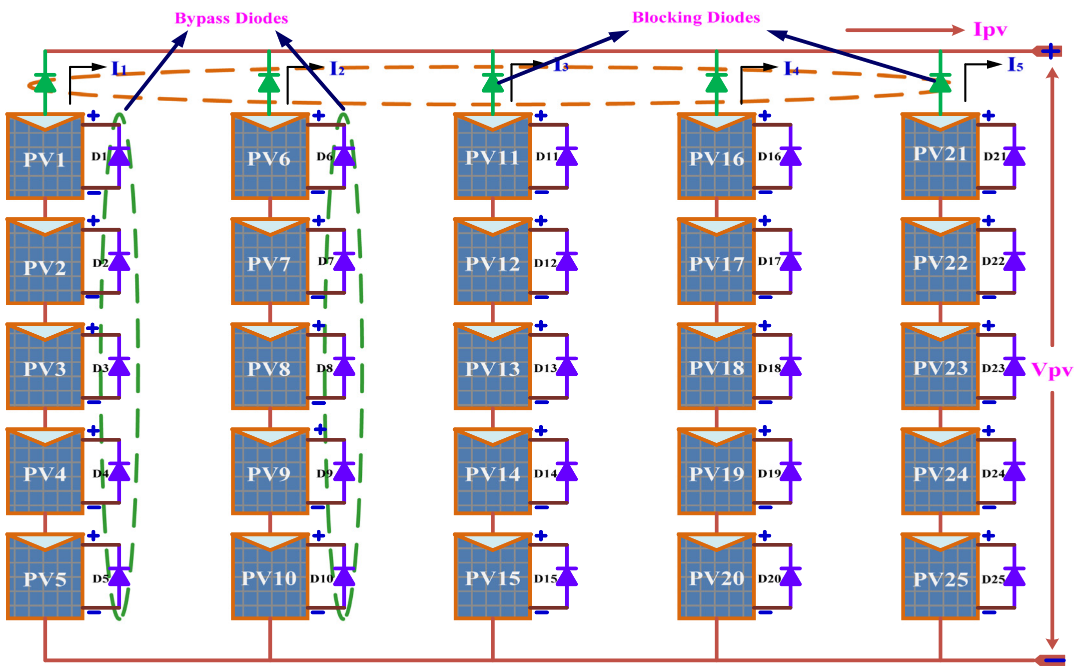


**Fig. 4a.** MATLAB/Simulink model of 5 × 5 Series–Parallel (S–P) PV array configuration.

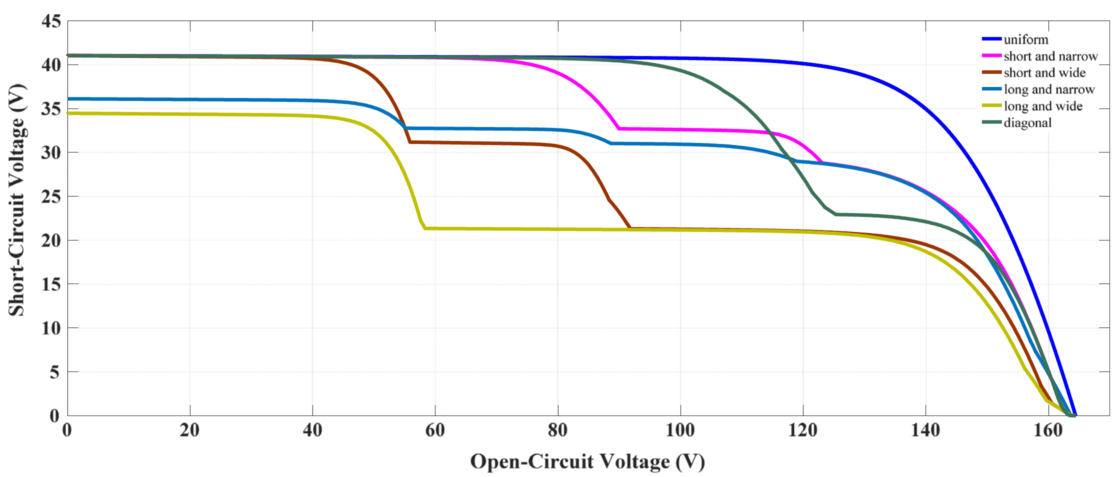


**Fig. 4b.** Simulated *I*–*V* characteristics of Series–Parallel (S–P) PV array configuration.

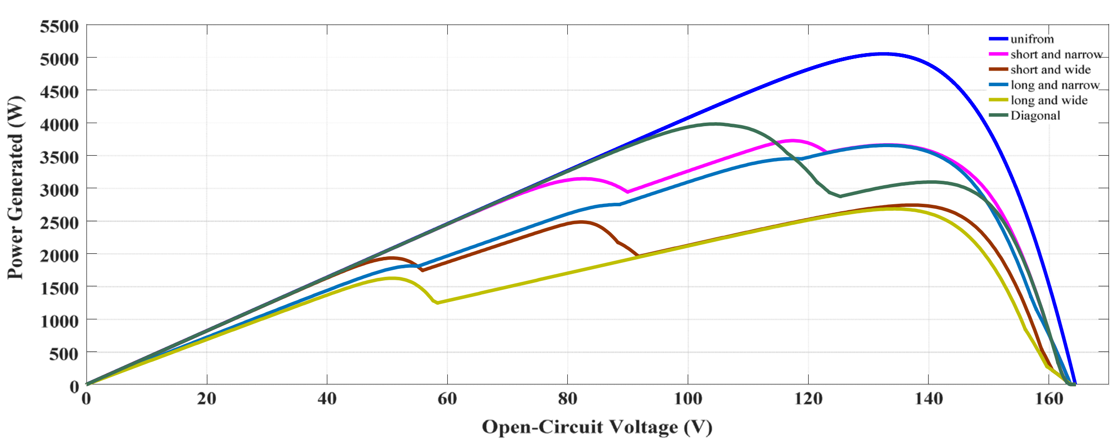


**Fig. 4c.** Simulated *P*–*V* characteristics of Series–Parallel (S–P) PV array configuration.

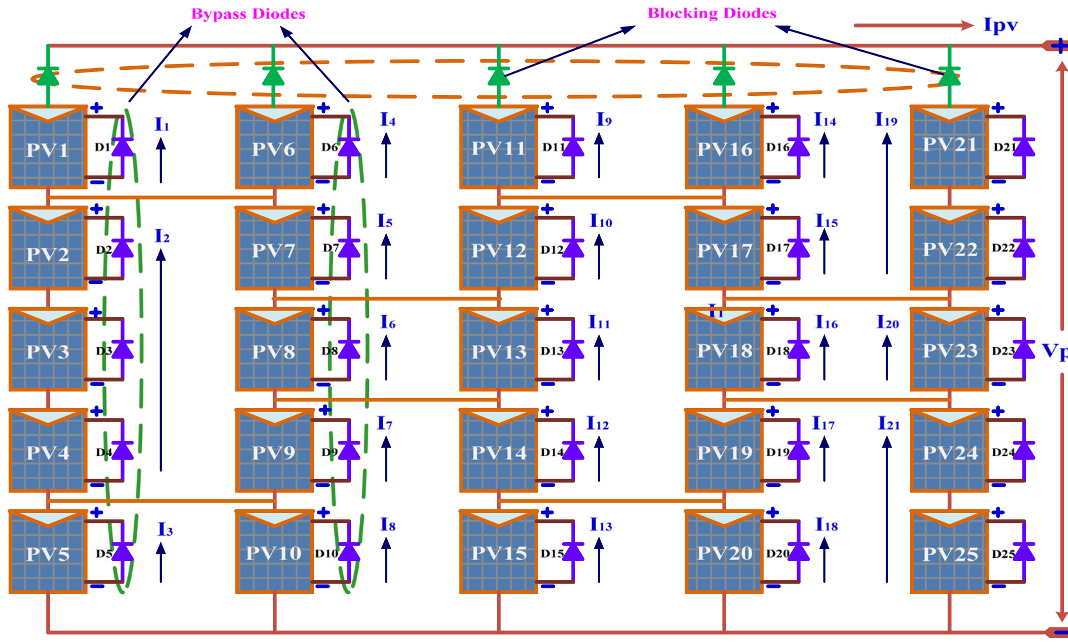


**Fig. 5a.** MATLAB/Simulink model of 5 × 5 Series–Parallel (S–P) PV array configuration.

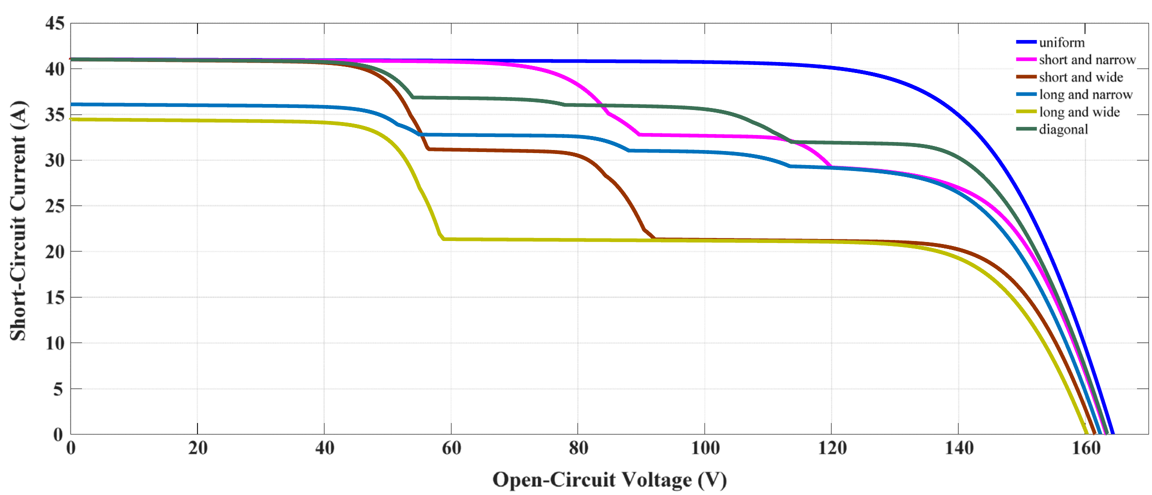


**Fig. 5b.** Simulated *I*–*V* characteristics of T–C–T PV array configuration under different PSCs.

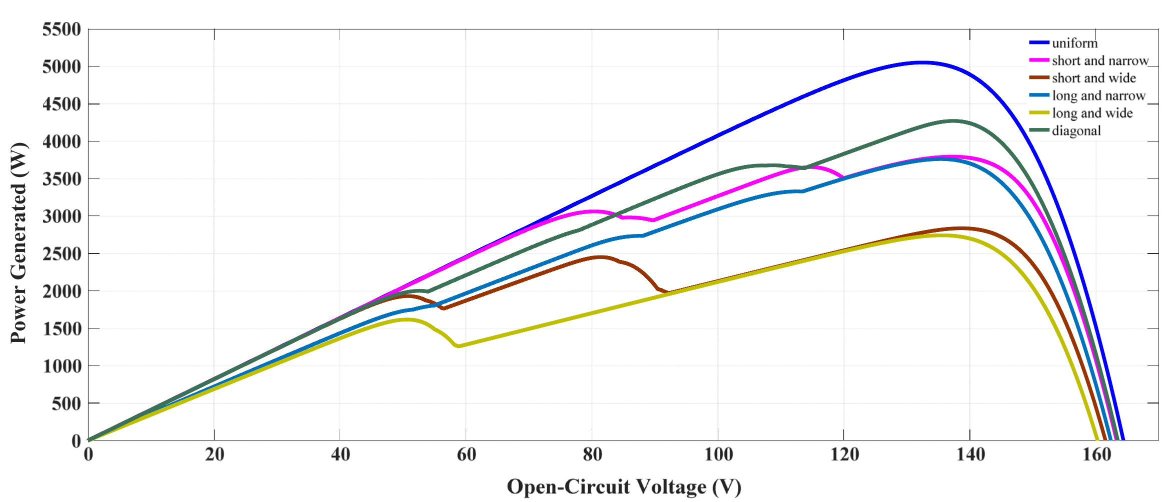


**Fig. 5c.** Simulated *P*–*V* characteristics of T–C–T PV array configuration under different PSCs.

**Table 6**
Expressions for the output current, voltage and power of PV array configurations.

| Topology | Output current [A] | Output voltage [V] | Output power [W] |
|---|---|---|---|
| **S** | $I_0 = I_J$ | $V_0 = \sum_{J=1}^{J=25} V_J = 25 \times V_J$ | $P_0 = V_0 \times I_0 = 25 \times V_J \times I_J$ |
| **S–P** | $I_0 = I_{S1} + I_{S2} + \cdots + I_{S5} = 5I_S$ | $V_0 = \sum_{J=1}^{J=5} V_J = 5V_J$ | $P_0 = V_0 \times I_0 = 25 \times V_J \times I_S$ |
| **H–C** | $I_0 = I_1 + I_4 + I_9 + I_{14} + I_{19} = 5I_S$ | $V_0 = \sum_{J=1}^{J=5} V_J = 5V_J$ | $P_0 = V_0 \times I_0 = 25 \times V_J \times I_S$ |

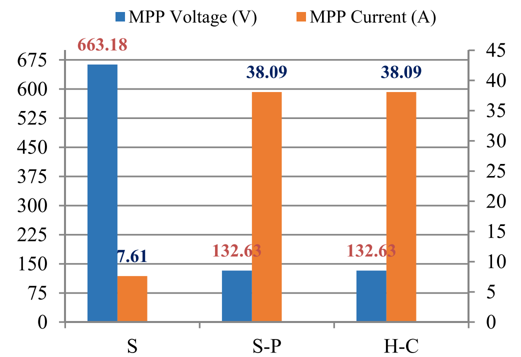


**Fig. 6a.** MPP voltages and currents under uniform irradiance condition.

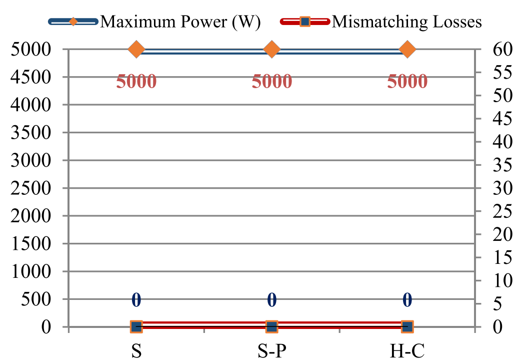


**Fig. 6b.** Maximum power and mismatching losses under uniform irradiance condition.

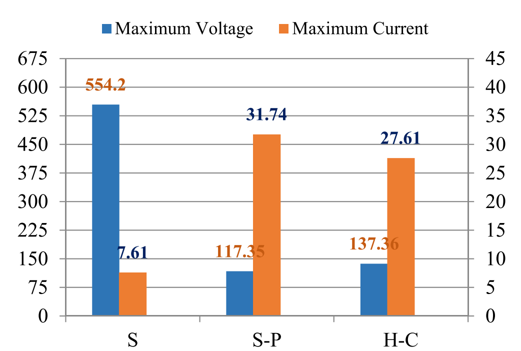


**Fig. 7a.** MPP voltages and currents under short and narrow shading condition.

power generated and mismatching losses produced by S, S–P and H-C array configurations are shown in Fig. 8b. The fill factors of these configurations are 0.39, 0.40 and 0.41 respectively. From the simulation results, under short and wide shading condition, it was observed that H-C configuration is the most appropriate configuration for generating the maximum power by reducing mismatching losses.

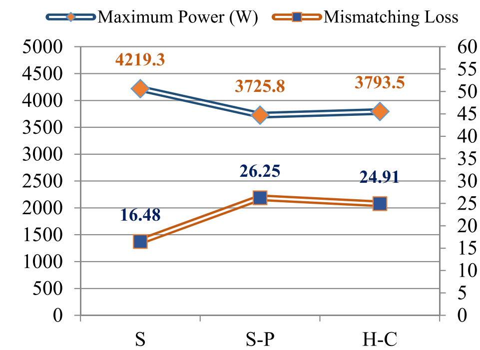


**Fig. 7b.** Maximum power and mismatching losses under short and narrow shading condition.

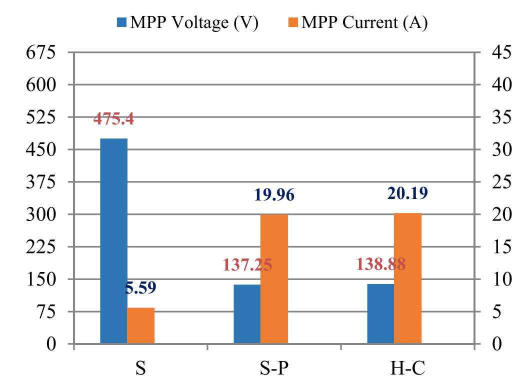


**Fig. 8a.** MPP voltages and currents under short and wide shading condition.

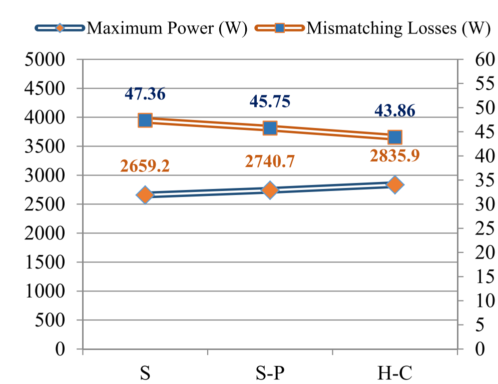


**Fig. 8b.** Maximum power and mismatching losses under short and wide shading condition.

### 5.2.3. *Long and narrow shading condition*

The generated maximum powers, voltages and currents of S, S–P and H-C array configurations under long and narrow shading condition are 3000.6 W, 535.2 V, 5.6 A; 3653.1 W, 133.18 V, 27.42 A and 3761.2 W, 135.48 V, 27.76 A respectively. Under this shading condition, H-C array configuration produces the highest maximum

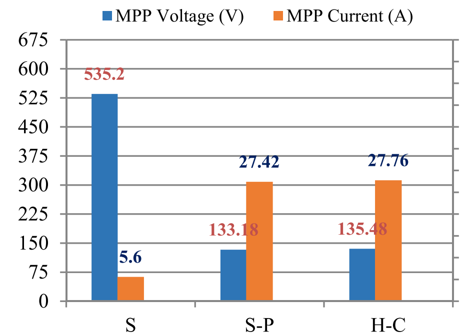


**Fig. 9a.** MPP voltages and currents under long and narrow irradiance condition.

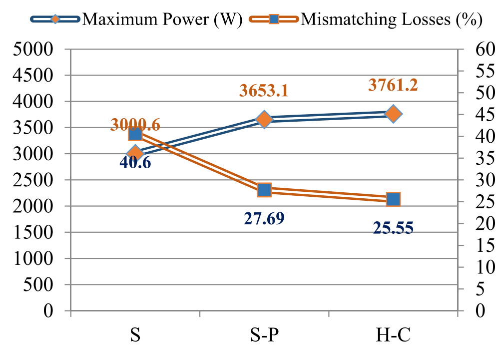


**Fig. 9b.** Maximum power and mismatching losses under long and narrow irradiance condition.

power of 3761.2 W by generating four MPPs on output characteristics as shown in Fig. 5c. The maximum generated voltages and currents of S, S–P and H-C configurations at MPP are shown in Fig. 9a. The mismatching losses produced by S, S–P and H-C array configurations are 40.6%, 27.69% and 25.55% respectively. The maximum power generated and mismatching losses produced by S, S–P and H-C array configurations are shown in Fig. 9b. The fill factors of S, S–P and H-C PV array configurations are 0.44, 0.54 and 0.55 respectively. From the simulation results, under long and narrow shading condition, it was examined that H-C configuration is the most appropriate configuration for generating the maximum power by reducing low mismatching losses.

### 5.2.4. Long and wide shading condition

The generated maximum powers, voltages and currents of S, S–P and H-C array configurations under long and wide shading condition are 2116.4 W, 533.47 V, 3.96 A; 2682 W, 134.04 V, 20.08 A and 2741.6 W, 135.78 V, 20.19 A respectively. Under this shading condition, H-C array configuration produces the highest maximum power of 2741.6 W by generating two MPPs on output characteristics as shown in Fig. 5c. The maximum generated voltages and currents of S, S–P and H-C configurations at MPP are shown in Fig. 10a. The mismatching losses produced by S, S–P and H-C array configurations are 58.1%, 46.91% and 45.73% respectively. The maximum power generated and mismatching losses produced by S, S–P and H-C array configurations are shown in Fig. 10b. The fill factors of these configurations are 0.31, 0.39 and 0.40 respectively. From the simulation results, under long and wide shading condition, it was inspected that H-C configuration is the most appropriate configuration for generating the maximum power by reducing mismatching losses.

### 5.2.5. Diagonal shading condition

The generated maximum powers, voltages and currents of S, S–P and H-C array configurations under diagonal shading condition

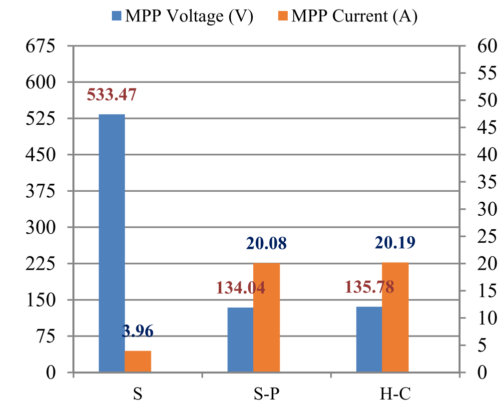


**Fig. 10a.** MPP voltages and currents under long and wide shading condition.

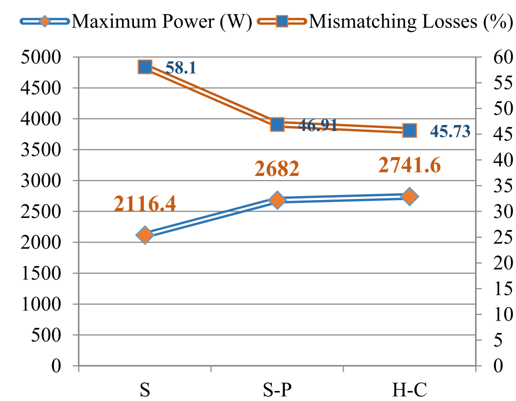


**Fig. 10b.** Maximum power and mismatching losses under long and wide shading condition.

are 4137.8 W, 568.18 V, 7.28 A; 3980.3 W, 104.61 V, 38.04 A and 4271.1 W, 137.49 V, 31.06 A respectively. Under this condition, H-C array configuration generates the highest maximum power of 4271.1 W by generating two MPPs on output characteristics as shown in Fig. 5c. The maximum generated voltages and currents of S, S–P and H-C configurations at MPP are shown in Fig. 11a. The mismatching losses produced by S, S–P and H-C array configurations are 18.09%, 21.21% and 15.46% respectively. The maximum power generated and mismatching losses produced by S, S–P and H-C array configurations are shown in Fig. 11b. The fill factors of these configurations are 0.61, 0.58 and 0.63 respectively. From the simulation results, under diagonal shading condition, it was observed that H-C configuration is the most appropriate configuration for generating the maximum power by reducing mismatching losses.

## 6. Conclusion

- This research article has investigated the performance of S, S–P and H- C PV array configurations by changing the electrical connections between the PV modules in a PV array that impacts the maximum power generation capability under different partial shading conditions; uniform, short and narrow, short and wide, long and narrow, long and wide, and diagonal shading condition.
- The output characteristics, i.e. *I–V* and *P–V* characteristics of S, S–P and H- C PV array configurations under above mentioned partial shading conditions are analyzed. From the simulation results, it is observed that when the number of

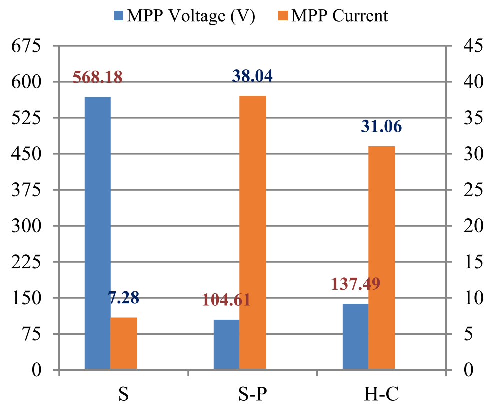


**Fig. 11a.** MPP voltages and currents under diagonal shading condition.

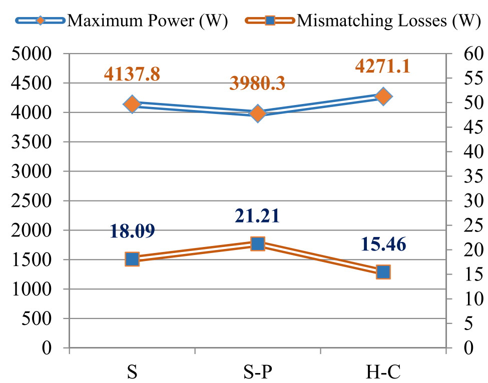


**Fig. 11b.** Maximum power and mismatching losses under diagonal shading condition.

PV modules are shaded per string and the number of strings shaded in a PV array increases, reduces the maximum power generation capability by causing mismatching power losses.

- It is observed that under short and narrow, short and wide, long and narrow, long and wide, and diagonal shading conditions; the S, S–P and H-C PV array configurations generates the maximum power and mismatching losses of 4219.3 W, 16.48%; 2835.9 W, 43.86%; 3761.2 W, 25.55%; 2741.6 W, 45.73%, and 4271.1 W, 15.46% respectively.
- It is also observed that, the S-array configuration generates the maximum power compared to S–P and H-C PV array configurations under short and narrow shading condition only. The S–P PV array configuration generates the maximum power compared to S-array configuration under short and wide, long and narrow, and long and wide shading condition only.
- The H-C PV array configuration generates the maximum power under all above mentioned shading conditions except in short and narrow shading condition. Therefore, from the MATLAB/ SIMULINK simulation results on S, S–P and H- C PV array configurations, it is concluded that in most of the partial shading conditions, the H-C PV array configuration is the most appropriate PV array configuration for the generation of maximum power compared to Series S and S–P PV array configurations.

## Acknowledgment

The Authors gratefully acknowledge the support offered by the Science and Engineering Research Board (SERB), Department of Science & Technology, Government of India under the Grant No: ECR/2017/000316 for this research work.

**Table A.1**
Parameters of KYOCERA-KC200GT PV module.

| S. No. | Parameters | Values |
|---|---|---|
| 1 | Maximum Power, $P_{max}$ | **200.143** W |
| 2 | Maximum Power Voltage, $V_{MP}$ | **26.3** V |
| 3 | Maximum Power Current, $I_{MP}$ | **7.61** A |
| 4 | Open Circuit Voltage, $V_{OC}$ | **32.9** V |
| 5 | Short Circuit Current, $I_{SC}$ | **8.21** A |
| 6 | Temperature co-efficient of open circuit voltage, $K_V$ | **−0.1230** V/K |
| 7 | Temperature co-efficient of short circuit current, $K_I$ | **0.0032** A/K |
| 8 | Number of cells per module, $n_s$ | **54** |
| 9 | Series Resistance, $R_S$ | **0.221** Ω |
| 10 | Shunt Resistance, $R_{SH}$ | **415.405** Ω |
| 11 | Diode ideality factor, $a$ | **1.3** |

## Appendix

Parameters of KYOCERA-KC200GT PV module are given in Table A.1.

## References

Ahmed, Jubaer, Salam, Zainal, 2015. A critical evaluation on maximum power point tracking methods for partial shading in PV systems. Renew. Sustain. Energy Rev. 47, 933–953.
Balato, M., et al., 2015. Series–Parallel PV array re-topology: Maximization of the extraction of energy and much more. Appl. Energy 159, 145–160.
Belhachat, F., Larbes, C., 2015. Modeling, analysis and comparison of solar photovoltaic array configurations under partial shading conditions. Sol. Energy 120, 399–418.
Bhatnagar, P., Nema, R.K., 2013. Maximum power point tracking control techniques: State-of-the-art in photovoltaic applications. Renew. Sustain. Energy Rev. 23, 224–241.
Chao, K.H., et al., 2015. The optimal configuration of photovoltaic module arrays based on adaptive switching controls. Energy Convers. Manage. 100, 157–167.
Cipriani, G., et al., 2014. Technical and economical comparison between different topologies of PV plant under mismatch effect. In: IEEE Int. Conference on Ecological Vehicles and Renewable Energies, EVER, pp. 1–6.
Dhople, S.V., et al., 2010. Multiple input boost converter to minimize power losses due to partial shading in photovoltaic modules. In: Proc. Energy Convers. Congr. Expo., pp.. 2633–2636.
Eltawil, Mohamed A., et al., 2013. MPPT topology for photovoltaic applications. Renew. Sustain. Energy Rev. 25, 793–813.
Essakiappan, Somasundaram, et al., 2011. Analysis and mitigation of common mode voltages in photovoltaic power systems. In: IEEE Int. Conference on Energy Conversion Congress and Exposition, ECCE, pp. 28-35.
Koutroulis, E., et al., 2012. A new technique for tracking the global maximum power point of PV arrays operating under partial-shading conditions. IEEE J. Photovolt. 2, 184–190.
Mäki, Anssi, et al., 2012. Operation of series-connected silicon-based photovoltaic modules under partial shading conditions. Prog. Photovolt. Res. Appl. 20, 298–309.
Manganiello, Patrizio, et al., 2015. Survey on mismatching and aging of PV modules: The closed loop. IEEE Trans. Ind. Electron. 62, 7276–7286.
Murtaza, Ali, et al., 2014. A maximum power point tracking topology based on bypass diode mechanism for PV arrays under partial shading conditions. Energy Build. 73, 13–25.
Patel, Hiren, Agarwal, Vivek, 2008. MATLAB-based modeling to study the effects of partial shading on PV array characteristics. IEEE Trans. Energy Convers. 23, 302–310.
Pongratananukul, N., et al., 2004. Tool for automated simulation of solar arrays using general-purpose simulators. In: IEEE Int. Conference on Computers in Power Electronics, pp. 10–14.
Quesada, G.V., et al., 2009. Electrical PV array reconfiguration strategy for energy extraction improvement in grid-connected PV systems. IEEE Trans. Ind. Electron. 56, 4319–4331.
Ramaprabha, R., Mathur, B.L., 2012. A comprehensive review and analysis of solar photovoltaic array configurations under partial shaded conditions. Int. J. Photoenergy 2012, 1–17.
Rani, B., et al., 2013. Enhanced power generation from PV array under partial shading conditions by shade dispersion using Su Do Ku configuration. IEEE Trans. Sustain. Energy 4, 594–601.

Roman, E., et al., 2006. Intelligent PV module for grid-connected PV systems. IEEE Trans. Ind. Electron 53, 1066–1073.
Verma, Deepak, et al., 2014. Maximum power point tracking (MPPT) topology: Recapitulation in solar photovoltaic systems. Renew. Sustain. Energy Rev. 54, 1018–1034.
Villalva, M.G., et al., 2009. Comprehensive approach to modeling and simulation of photovoltaic arrays. IEEE Trans. Power Electron. 24, 1198–1208.
Wang, Y.j., Hsu, P.C., 2011. An investigation on partial shading of PV modules with different connection configurations of PV cells. Energy 36, 3069–3078.